# Nonlocal effect of plasma resonances on the electron energy-distribution function in microwave plasma columns

O. Boudreault, S. Mattei, L. Stafford,[*] J. Margot, and M. Moisan

*Département de Physique, Université de Montréal, Montréal, Québec, Canada H3C 3J7*

R. Khare and V. M. Donnelly

*Departement of Chemical and Biomolecular Engineering, University of Houston, Houston, Texas 77204, USA*

Spatially resolved trace rare gases optical emission spectroscopy was used to analyze the electron energy-distribution function (EEDF) in low-pressure argon plasma columns sustained by surface waves. At frequencies >1 GHz, in the microwave-sustained region, the EEDF departs from a Maxwellian, characterized by a depletion of low-energy electrons and a high-energy tail, whereas in the field-free zone, the EEDF is Maxwellian. Abnormal behavior of the EEDF results from the acceleration of low-energy electrons due to the conversion of surface waves into volume plasmons at the resonance point where the plasma frequency equals the wave frequency and their absorption by either collisional or Landau damping.

Recent advances in large-area plasma sources sustained by microwave electromagnetic (EM) fields, intended for various technological applications (e.g., etching and deposition of thin films), have raised many questions on the physics driving electron heating and wave-particle interactions in such discharges. In general, electrons in high-frequency plasmas are accelerated by the electric field and energy is redistributed to the plasma particles through electron-neutral collisions. In the near-collisionless regime where the frequency for electron-neutral collisions $\nu$ is much lower than the field angular frequency $\omega$, electron heating can also result from momentum transfer from high-voltage moving sheaths [1–3]. This stochastic electron heating is particularly important in plasmas created and maintained by a radio-frequency electric field not exhibiting a wave nature (plasma dimensions much smaller than the wavelength), such as capacitively coupled plasmas. On the other hand, when the electric field supporting the plasma is an EM wave (e.g., a surface wave) that carries the power away from the wave launching region [4,5], the self-consistent interaction between the wave and the plasma results in an overdense discharge (i.e., electron angular plasma frequency $\omega_{pe}$ higher than $\omega$) that can give rise to a number of interesting phenomena, including modulation instability and possibilities of soliton formation [6], wave breaking [7], and electron cyclotron resonance [8]. A few studies further pointed out the development of electron plasma resonances near the discharge boundaries where $\omega \approx \omega_{pe}$, resulting from the spatial inhomogeneity of the plasma [9]. These resonances result in large and sharp peaks of the electric field component parallel to the density gradient [10–12]. On the basis of hydrodynamic and kinetic calculations, it was proposed that the enhancement of the electric field could result in enhanced Joule heating [10] as well as the generation of fast electrons [13].

The existence and precise role of plasma resonances nonetheless continues to be a subject of debate, due to a lack of convincing and comprehensive experimental validation [14]. Indirect evidence by Langmuir probe measurements has been reported, such as the presence of local peaks in the plasma-floating potential near the end of a plasma column [15], and the detection of high-energy electrons near the fused-silica windows in both tubular and planar-type surface-wave discharges [16–19]. It is well known, however, that probe measurements are problematic in wave-sustained plasmas since metallic electrodes perturb the self-consistent wave-plasma behavior. In addition, the contribution of high-energy electrons to the total probe current is hindered by a large ion current.

In this Rapid Communication, a nonintrusive, trace rare gases optical emission spectroscopy (TRG-OES) technique that is highly sensitive to the detection of high-energy electrons is used to analyze the electron energy-distribution function (EEDF) along a low-pressure argon plasma column sustained in the microwave regime by EM surface waves. In the large-area, planar-type configurations used in many industry-driven applications, the EM field is stationary and often exhibits a multimode behavior, making fundamental investigations of the physics driving the electron dynamics difficult due to the complexity of the corresponding field distribution. In contrast, in the long, tubular configuration used in this study, the wave is a traveling wave and monomode propagation is readily achievable [20]. From our spatially resolved measurements of the EEDF performed over a wide range of frequencies, it is concluded that the nonlocal electron dynamics in the overdense region of surface-wave plasmas is strongly linked to the excitation of volume plasmons near the discharge boundary at the resonance point where $\omega_p = \omega$ and their absorption by either collisional or Landau damping.

Most of our experiments were carried out in a 6 mm inner diameter (i.d.) fused-silica discharge tube evacuated by a turbomolecular pump. As detailed below, selected experiments were also performed in a fused-silica tube tapering up from 6 to 25 mm i.d. In both systems, the EM surface wave was excited in the small portion of the tube, using a gap-type wave launcher. A surfatron device [21] was used for experiments in

---

[*]Corresponding author: luc.stafford@umontreal.ca

the 600–2450 MHz frequency range while a Ro-box unit [22] was utilized to sustain plasmas at lower frequencies. The product of the frequency $f$ times the tube radius $R$ was always $\ll 2$ GHz cm, therefore ensuring that only the azimuthally symmetric mode of wave propagation (i.e., the mode for which the EM wave field intensity does not vary azimuthally) could be excited [20]. An argon flow rate of 20 standard cubic centimeters per minute (sccm) was mixed with 1 sccm of rare gases contained in a premixed-gas bottle (40% Ne and 20% each for Ar, Kr, and Xe) to allow TRG-OES measurements. Plasma emission was collected by an optical fiber equipped with a collimator directed perpendicularly to the discharge tube axis, and monitored using an intensity-calibrated optical spectrometer.

In TRG-OES, the electron temperature is determined by measuring the emission line intensities coming from the $2p_x$ levels (Paschen's notation) of rare gases (here Ne, Kr, and Xe) inserted in trace amounts, and comparing them to values computed from a model using the known electron-impact cross sections and branching ratios [23]. By selecting appropriate emission lines, an electron "temperature" characterizing an assumed Maxwellian distribution in a specific electron energy range can be determined for different energy segments of the EEDF. Three groups of emission lines were considered in this study, leading to three temperatures designated as low, high, and tail. The first one, $T_e^{\text{low}}$, was obtained using a set of five Kr and Xe lines that are mainly excited by electron impact from the $^3P_{0,2}$ metastable levels (see Ref. [23]). The difference in energy between these metastable states and the emitting $2p_x$ levels being only of a few eV, $T_e^{\text{low}}$ is thus representative of the low-energy portion of the EEDF. $T_e^{\text{high}}$ was determined using a set of six lines from Kr and Xe for which the upper levels are populated mainly by electron-impact excitation directly from the ground states (see Ref. [23]), requiring electron energies of $>9.6$–$12.3$ eV, i.e., the high-energy part of the EEDF. Finally, the high-energy tail of the EEDF was represented by a "tail temperature" $T_e^{\text{tail}}$ determined using the same emission lines as for $T_e^{\text{high}}$ but with the addition of the Ne $2p^{10}$-$1s^4$ transition at 585.2 nm (the energy of the Ne $2p^{10}$ level is 19 eV above ground state and the contribution from stepwise excitation from the metastable states is negligible). Since Ar was the main plasma gas, none of its very intense emission lines were used due to radiation trapping effects [24]. If the EEDFs were truly Maxwellian, then the use of different sets of emission lines gives an identical electron temperature. On the other hand, if different electron temperatures are found, then it is possible to determine how the EEDF departs from a Maxwellian.

Figure 1 shows the electron temperatures for a 50 mTorr argon plasma column. For $f = 100$ MHz, $T_e^{\text{low}} \approx T_e^{\text{high}} \approx T_e^{\text{tail}} \simeq 4$ eV, suggesting that the EEDF is a Maxwellian. On the other hand, as the EM field frequency increases, both $T_e^{\text{low}}$ and $T_e^{\text{tail}}$ increase while $T_e^{\text{high}}$ remains constant. At microwave frequencies, the EEDF thus has a distinct, three-temperature form with a steeper slope for the energy segments concerning low-energy electrons ($T_e^{\text{low}} > T_e^{\text{high}}$) and very high-energy electrons ($T_e^{\text{tail}} > T_e^{\text{high}}$). Hence, even with the relatively high ionization degree ($\sim 1\%$) achieved in microwave-sustained plasmas, electron-electron collisions appear insufficient to ensure a Maxwellian distribution [25].
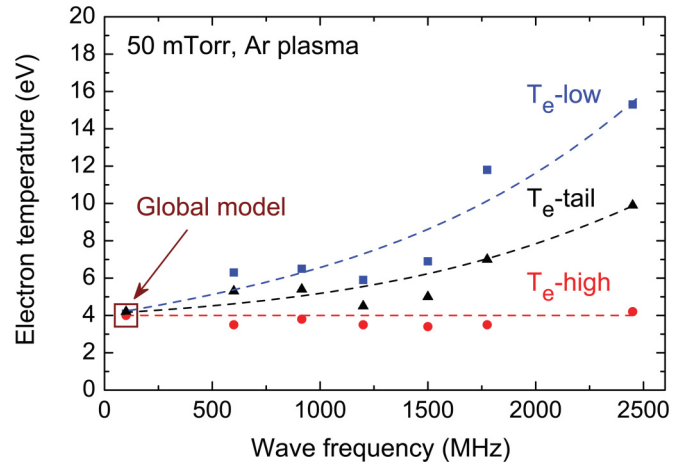


FIG. 1. (Color online) Influence of the wave frequency on the values of $T_e^{\text{low}}$, $T_e^{\text{high}}$, and $T_e^{\text{tail}}$ determined by TRG-OES in a 50 mTorr Ar plasma column sustained by surface waves at 4 cm from the end of the plasma column.

The average electron temperature $\langle T_e \rangle$ can be calculated using a zero-dimensional model assuming that charged particles are created by electron-impact ionization on the ground state and are lost by ambipolar diffusion to the reactor walls. With this reasonable assumption for plasmas operated in the mTorr pressure range, the electron temperature depends only on the discharge gas pressure and nature and on plasma dimensions, yielding [26]

$$T_e = \frac{E_{iz}}{\ln(n_g \Lambda A_{iz}/u_B)}, \tag{1}$$

where $E_{iz}$ and $A_{iz}$ are parameters in the expression for the ionization rate coefficient $k = A_{iz} \exp(-E_{iz}/T_e)$, $n_g$ is the neutral gas number density, $u_B$ is the Bohm velocity, and $\Lambda$ is an effective plasma length for positive ion diffusion given by $(1/\Lambda)^2 = (\pi/L)^2 + (2.405/R)^2$ for a cylindrical tube of length $L$ and radius $R$. For a 50 mTorr Ar plasma with $L \gg R = 3$ mm, $T_e = 4$ eV, consistent with the data in Fig. 1 at low operating frequencies. Even though the "temperature" of the electrons in the intermediate range of energy $T_e^{\text{high}}$ remains more or less constant from 100 MHz to 2.45 GHz, one still expects higher average electron energies at high operating frequencies from the increase of the other two characteristic temperatures (Fig. 1). From the measurements of $T_e^{\text{low}}$, $T_e^{\text{high}}$, and $T_e^{\text{tail}}$, it is, however, difficult to construct the full EEDF with enough precision to determine whether the mean electron energy satisfies Eq. (1) at all frequencies. Nonetheless, by doing so, using the approach in Ref. [27], we obtained a $\langle T_e \rangle$ value of 5–6 eV at 2.45 GHz. The slightly higher mean electron energies can probably be explained by a depletion of the number density of Ar neutrals available for ionization, due to the much higher electron densities at 2.45 GHz than at 100 MHz. For example, for $\langle T_e \rangle = 6$ eV and a typical radially integrated electron number density of $3 \times 10^{12}$ cm$^{-3}$ along the surface-wave argon plasma column at 2.45 GHz, the electron pressure accounts for 25% of the total pressure, reducing the neutral atom pressure to 35 mTorr (we assume a neutral gas temperature of 300 K [28]). Given the corresponding 25% reduction in $n_g$, Eq. (1) predicts $\langle T_e \rangle = 5$ eV, consistent with

our approximate averaging over the three energy segments of 5–6 eV at 2.45 GHz.

The data presented in Fig. 1 further suggests that raising the wave frequency induces a depletion in the number of low-energy electrons with respect to a single Maxwellian of $T_e = 4$ eV ($T_e^{low} > T_e^{high}$) as well as the generation of fast electrons ($T_e^{tail} > T_e^{high}$). Several mechanisms can induce abnormal electron heating, thus yielding a non-Maxwellian EEDF. Stochastic electron heating due to oscillating plasma sheaths cannot be invoked in microwave discharges: For the sheath to oscillate, the characteristic time for the sheath formation ($\sim 2\pi/\omega_{pe}$) must be much shorter than the wave period $T = 2\pi/\omega$. While this is the case in radio-frequency plasmas ($\omega/\omega_{pe} \sim 500$ at 13.56 MHz), the time for sheath formation in microwave discharges is at most comparable to, but not much shorter than, the wave period. Since the wave oscillations are too fast for the sheath to follow, there should be no significant stochastic heating related to sheath oscillations. In addition, in the microwave regime, the excursion lengths of the electrons per oscillating cycle are generally much smaller than the plasma dimensions. On the other hand, given the high number densities of electrons ($\sim 10^{12}$ cm$^{-3}$) and Ar atoms in metastable and resonant states ($\sim 10^{12}$ cm$^{-3}$) in 2.45 GHz plasmas, one might expect superelastic collisions to play an important role in electron heating. This possibility was investigated through kinetic simulations using the Boltzmann code provided by Hagelaar and Pitchford [29]. As shown in Fig. 2, even multiplying the cross sections for superelastic collisions by a factor of 100 with respect to published values introduces only small changes in the EEDF.

As mentioned above, the presence of high-intensity electric fields near the discharge boundaries in spatially inhomogeneous surface-wave plasmas due to the development of electron plasma resonances at $\omega \approx \omega_{pe}$ was theoretically predicted to produce suprathermal electrons [13]. This could possibly be attributed to transit-time heating during the electron transit time $\tau$ across the resonance peak of width $\Delta$ [10,16]. Transit-time heating occurs mostly when $\omega\tau \approx 1$

(for $\omega\tau \gg 1$, the electron oscillates in the field without gaining energy until a collision disrupts its oscillation, while for $\omega\tau \ll 1$ the electron is traveling too fast to experience the resonant field) [30]. For $\omega = 2\pi \times 2.45$ GHz and an estimated resonance width $\Delta = 2 \times 10^{-4}$ cm [10] for a 50 mTorr Ar plasma with a radially integrated electron number density of $10^{12}$ cm$^{-3}$, this criterion corresponds to an electron velocity $u = \omega\Delta = 3 \times 10^6$ cm s$^{-1}$, i.e., an electron energy of 2.5 meV. Consequently, only very low-energy electrons could eventually be accelerated to a tenth of eV, indicating that transit-time heating through the resonant layer cannot explain the depletion of low-energy electrons in the few eV range described by $T_e^{low}$ and the generation of electrons in the tens of eV given by $T_e^{tail}$.

As theoretically proposed by Aliev *et al.* [31], fast electron generation could result from the resonant conversion of long-wavelength electromagnetic surface waves into short-wavelength electrostatic Langmuir waves (volume plasmons) and their absorption by either collisional or Landau damping. To play an important role, these waves would need wavelengths much smaller than the plasma diameter, i.e., $\sim 0.1$–0.6 mm for our conditions. For $f = 2.45$ GHz, this corresponds to phase velocities in the 2–15 $\times 10^7$ cm s$^{-1}$ range and thus to electron energies between 0.1 and 6 eV. These low-energy electrons could therefore be accelerated to form the high-energy tail seen in the experiments. On the other hand, for $f = 100$ MHz, if a similar resonant conversion occurred, the corresponding phase velocities would be 1–6 $\times 10^6$ cm s$^{-1}$, i.e., much lower electron energies. Similarly to transit-time heating, this would play only a minor role in the electron dynamics, which again is consistent with our experimental observations. In addition, at lower frequencies, the plasma tends to become more collisional ($\nu/\omega$ increases) such that the resonance is less pronounced and thus resonant wave conversion less likely [32].

Figure 3 presents the radial profile of $T_e^{low}$, $T_e^{high}$, and $T_e^{tail}$ obtained from the laterally resolved optical emission spectra after Abel inversion. Despite the localized character of the electron plasma resonance, all values of $T_e$ are radially uniform. This is in sharp contrast to the common local field
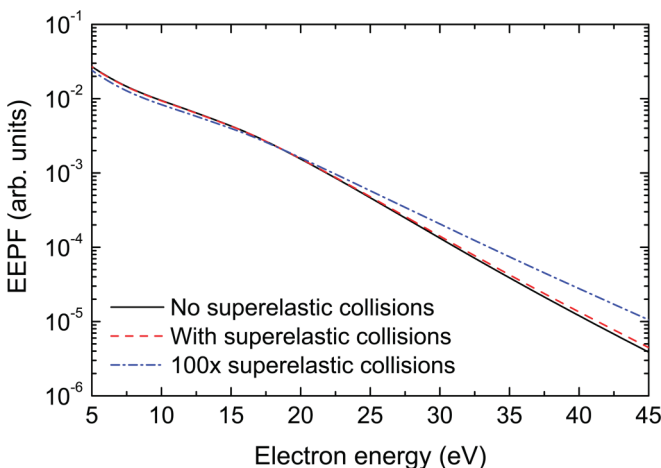


FIG. 2. (Color online) Influence of superelastic collisions on the electron energy probability function (EEPF) determined by kinetic simulations.
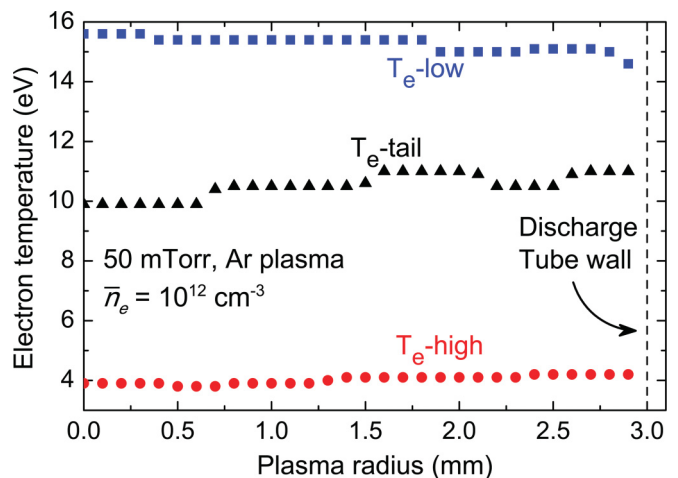


FIG. 3. (Color online) Radial profiles of $T_e^{low}$, $T_e^{high}$, and $T_e^{tail}$ determined by TRG-OES in a 50 mTorr Ar plasma column sustained by surface waves at 2.45 GHz.
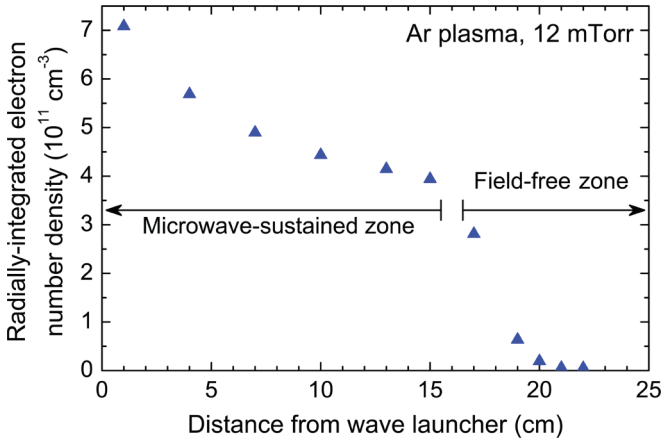
FIG. 4. (Color online) Axial profile of the line-integrated electron number density in a 12 mTorr Ar plasma column sustained by surface waves at 2.45 GHz. Measurements were performed in the larger portion of a tapered fused-silica discharge tube. Electron densities were obtained from phase-sensitive microwave interferometry in the microwave-sustained region and optical emission spectroscopy in the field-free zone (see Ref. [28] for details).

TABLE I. Comparison of the electron temperatures determined by TRG-OES in the large portion of the tapered tube for a 2.45 GHz Ar plasma column.

| $T_e$ | Overdense plasma (eV) | Expansion region (eV) |
|---|---|---|
| $T_e^{\mathrm{low}}$ | 7.9 | 3.9 |
| $T_e^{\mathrm{high}}$ | 4.3 | 4.4 |
| $T_e^{\mathrm{tail}}$ | 7.9 | 4.4 |

approximation in which fast electron generation should be limited to the resonance region, i.e., close to the discharge boundaries. In the low-pressure conditions investigated here, however, since the energy relaxation length of electrons ($\sim$2 cm for electrons of average speed $10^8$ cm/s and an electron-neutral collision frequency of $2 \times 10^8$ s$^{-1}$ in the 50 mTorr Ar plasma) is larger than the radial size of the reactor (0.6 cm) and of the scale lengths of the spatial inhomogeneity ($\Delta = 2 \times 10^{-4}$ cm), energy transport effects play a crucial role. In such conditions, the local energy absorption by the electrons going through the plasma resonance is redistributed over the whole plasma volume (nonlocal effect) [33].

To further confirm the precise role of localized plasma resonances on the evolution of the nonlocal EEDF, TRG-OES measurements were performed for conditions where no surface-wave electric fields are present and thus where no resonance conversion occurs. For surface-wave plasmas sustained in long and narrow dielectric tubes, the electron density decreases along the tube's $z$ axis down to the lowest density for which surface-wave propagation is allowed [34]. Beyond this critical point, a field-free region exists in which the plasma decays more or less abruptly to zero due to diffusion and convection [28]. In the 50 mTorr, 6 mm i.d. plasma column examined, this field-free region was too short to allow detailed TRG-OES investigations. To circumvent this limitation, a tapered, fused-silica discharge tube was used. The plasma was sustain in the small 6 mm diam segment to ensure that only the azimuthally symmetric surface wave could be excited while plasma emissions were recorded in the large 25 mm

diam region. To maintain the same $n_g\Lambda$ scale factor and thus the same mean electron energy as in the previous experiments [see Eq. (1)], the pressure was reduced to 12 mTorr. The axial distribution of the radially integrated electron number density is presented in Fig. 4 for $f = 2.45$ GHz. TRG-OES measurements were performed both in the microwave-sustained region (within this larger diameter tube) and far in the field-free zone. The corresponding values of $T_e^{\mathrm{low}}$, $T_e^{\mathrm{high}}$, and $T_e^{\mathrm{tail}}$ are presented in Table I. In the absence of the surface-wave electric field, the EEDF was close to a Maxwellian with $T_e^{\mathrm{low}} \approx T_e^{\mathrm{high}} \approx T_e^{\mathrm{tail}} \simeq 4$ eV. On the other hand, in the microwave-sustained region where localized resonant effects occur, the EDDF show again a departure from a Maxwellian of temperature $\langle T_e \rangle = 4$ eV with a depletion of low-energy electrons given by $T_e^{\mathrm{low}}$ and fast electron generation given by $T_e^{\mathrm{tail}}$.

In summary, nonlocal electron heating of low-energy electrons was observed in low-pressure argon plasma columns sustained in the microwave regime by electromagnetic surface waves which can be explained by the presence of a plasma resonance near the discharge boundaries. As shown in this Rapid Communication, the effect of resonances in the spatially inhomogeneous plasma appears primarily in the form of a depletion of low-energy electrons due to their acceleration. Electron heating can be ascribed to a wave-particle interaction due to the conversion of surface waves into volume plasmons at the resonance point rather than transit-time electron heating across the resonant layer. The present work represents strong experimental evidence of the nonlocal role of plasma resonances on the EEDF in spatially inhomogeneous and weakly collisional microwave discharges. Future plasma modeling studies of low-pressure microwave discharges should therefore rely on an exhaustive, non-local kinetic treatment accounting for the effects of plasma resonance on the abnormal evolution of the EEDF.

[1] J. Y. Hsu, K. Matsuda, M. S. Chu, and T. H. Jensen, Phys. Rev. Lett. **43**, 203 (1979).

[2] M. M. Turner, Phys. Rev. Lett. **75**, 1312 (1995).

[3] G. Gozadinos, M. M. Turner, and D. Vender, Phys. Rev. Lett. **87**, 135004 (2001).

[4] I. Odrobina, J. Kudela, and M. Kando, Plasma Sources Sci. Technol. **7**, 238 (1998).

[5] M. Moisan, A. Shivarova, and A. W. Trivelpiece, Plasma Phys. **24**, 1331 (1982).

[6] D. Grozev, K. Kirov, K. Makasheva, and A. Shivarova, IEEE Trans. Plasma Sci. **25**, 415 (1997).

[7] A. Y. Lee, Y. Nishida, N. C. Luhmann Jr., S. P. Obenschain, B. Gu, M. Rhodes, J. R. Albritton, and E. A. Williams, Phys. Rev. Lett. **48**, 319 (1982).

[8] J. Margot and M. Moisan, J. Phys. D: Appl. Phys. **24**, 1765 (1991).

[9] I. Ghanashev, H. Sugai, S. Morita, and N. Toyoda, Plasma Sources Sci. Technol. **8**, 363 (1999).

[10] L. L. Alves, S. Letout, and C. Boisse-Laporte, Phys. Rev. E **79**, 016403 (2009).

[11] Y. M. Aliev, J. Berndt, H. Schlüter, and A. Shivarova, Plasma Phys. Controlled Fusion **36**, 937 (1994).

[12] T. Terebessy, M. Siry, M. Kando, J. Kudela, and D. Korsec, Appl. Phys. Lett. **77**, 2825 (2000).

[13] Y. M. Aliev, V. Y. Bychenkov, A. V. Maximov, and H. Schlüter, Plasma Sources Sci. Technol. **1**, 126 (1992).

[14] I. P. Ganashev and H. Sugai, Plasma Sources Sci. Technol. **11**, A178 (2002).

[15] A. Durandet, Y. Arnal, J. Margot-Chaker, and M. Moisan, J. Phys. D: Appl. Phys. **22**, 1288 (1989).

[16] S. Letout, C. Boisse-Laporte, and L. L. Alves, Appl. Phys. Lett. **89**, 241502 (2006).

[17] J. Kudela, T. Terebessy, and M. Kando, Appl. Phys. Lett. **76**, 1249 (2000).

[18] M. Nagatsu, T. Niwa, and H. Sugai, Appl. Phys. Lett. **81**, 1966 (2002).

[19] S. Nakao, E. Stamate, and H. Sugai, Thin Solid Films **515**, 4869 (2007).

[20] J. Margot-Chaker, M. Moisan, M. Chaker, V. M. M. Glaude, P. Lauque, J. Paraszczak, and G. Sauvé, J. Appl. Phys. **66**, 4134 (1989).

[21] M. Moisan, Z. Zakrzewski, and R. Pantel, J. Phys. D: Appl. Phys. **12**, 219 (1979).

[22] M. Moisan and Z. Zakrzewski, Rev. Sci. Instrum. **58**, 1895 (1987).

[23] V. M. Donnelly, J. Phys. D: Appl. Phys. **37**, R217 (2004).

[24] M. J. Schabel, V. M. Donnelly, A. Kornblit, and W. W. Tai, J. Vac. Sci. Technol. A **20**, 555 (2002).

[25] U. Kortshagen and H. Schlüter, J. Phys. D: Appl. Phys. **25**, 644 (1992).

[26] M. A. Lieberman and A. J. Lichtenberg, *Principles of Plasma Discharges and Materials Processing* (Wiley, New York, 1994).

[27] V. M. Donnelly and M. J. Schabel, J. Appl. Phys. **91**, 6288 (2002).

[28] S. Mattei, O. Boudreault, R. Khare, L. Stafford, and V. M. Donnelly, J. Appl. Phys. **109**, 113304 (2011).

[29] G. J. M. Hagelaar and L. C. Pitchford, Plasma Sources Sci. Technol. **14**, 722 (2005).

[30] V. A. Godyak and V. I. Kolobov, Phys. Rev. Lett. **81**, 369 (1998).

[31] Y. M. Aliev, A. V. Maximov, and H. Schlüter, Phys. Scr. **48**, 464 (1993)

[32] J. Margot and M. Moisan, J. Plasma Phys. **49**, 357 (1993).

[33] I. D. Kaganovich, V. I. Demidov, S. F. Adams, and Y. Raitses, Plasma Phys. Controlled Fusion **51**, 124003 (2009).

[34] V. M. M. Glaude, M. Moisan, R. Pantel, P. Leprince, and J. Marec, J. Appl. Phys. **51**, 5693 (1981).